*Inorg. Chem.* **2003**, *42*, 7290–7296


# Unusual Coordination Assemblies from Platinum(II) Thienyl and Bithienyl Complexes

**Peili Teo, L. L. Koh, and T. S. Andy Hor***

*Department of Chemistry, National University of Singapore, 3 Science Drive 3, Singapore 117543*

Received June 18, 2003

Dinuclear $Pt_2Br_2(dppf)_2(\mu\text{-}C_8H_4S_2)$ exchanges with isonicotinic acid to release free bithiophene and gives a molecular square $[Pt_4(dppf)_4(\mu_2\text{-}O_2CC_5H_4N)_4]^{4+}4OTf^-$ which is an "all-ring" system with four Pt rings disposed at the corners of a larger macrocyclic ring. The related mononuclear complex $PtBr(\eta^1(C2)\text{-}C_4H_3S)(dppf)$ reacts with AgOTf (OTf = triflate) to give $[Pt_2(dppf)_2(\mu_2,\eta^1(C),\eta^1(S)\text{-}C_4H_3S)_2]^{2+}2OTf^-$ with an unusual six-membered ring formed by the fusion of two Pt–thienyl entities at the sulfur sites. All the complexes are structurally characterized by single-crystal X-ray crystallography.

## Introduction

A key challenge facing the future of nanotechnology is molecular manufacturing, a process that is designed to synthesize advanced materials with targeted properties and functions.[1] Over the past decade, the use of metal coordination as a means to drive and preserve the formation of discrete molecular ensembles has become a methodology of emerging significance in supramolecular chemistry.[1] The metal polymers thus formed are often electroactive and conducting, and very importantly, they are potential candidates for a new generation of polymers that have both classical (e.g., mechanical and processing advantages) and contemporary (e.g., optical and semiconducting behaviors) functions and strengths.[2] Some recent uses of electroactive spacers such as bipyridine and functional groups such as ferrocene in metal-containing polymers are typical of such examples.[3−5] Our current interest in Pt(II)−thienyl and −bithienyl chemistry is developed along a similar vein as these complexes are generally redox-[6] and electroactive.[7,8] In this paper, we illustrate the construction of molecular entities with specific geometrical patterns, demonstrate that the (bi)thienyl entity can be retained or replaced, depending on conditions, and describe the unusual features of the products thus obtained.

## Results and Discussion

The $PPh_3$ thienyl and bithienyl complexes have been reported.[6] Replacement of $PPh_3$ by a flexible and functional 1,1′-bis(diphenylphosphino)ferrocene (dppf)[9] in the syntheses led to the isolation of the analogous dppf complexes, viz. $PtBr(C_4H_3S)(dppf)$, **1**, and $Pt_2Br_2(dppf)_2(\mu_2\text{-}C_8H_4S_2)$, **2**, in good yields (ca. 80%, 87%, respectively). The $^{31}P$ NMR spectrum of **2** shows two discrete resonances ($\delta$ 13.6, 12.7 ppm), corresponding to two phosphine centers opposite two different ligands, viz. bithienyl and bromide. The significantly lower $\pi$-acidity of bromide (compared to bithienyl) gives a much higher (by ca. 50%) Pt−P coupling for the *trans*-phosphine.[10] This, together with the $^1H$ NMR data of the bithienyl group, pointed to a dinuclear complex with two Pt(II)-chelating dppf entities bridged by a bithienyl group. Crystallographic analysis of **2** confirmed this proposition with terminal bromide completing a dinuclear core (Figure 2, Table 1). As expected, the bithienyl bridge is C-coordinated with free S sites. The Pt−P bond *trans* to bromide (2.232-

* To whom correspondence should be addressed. E-mail: andyhor@nus.edu.sg.

(1) Jean, J. M. *Supramolecular Chemistry, Concepts and Perspectives*; VCH: Weinheim, 1995.
(2) Heeger, A. J. *Synth. Met.* **2002**, *125*, 23.
(3) Biani, F. D.; Jackle, F.; Spiegler, M.; Wagner, M.; Zanello, P. *Inorg. Chem.* **1997**, *36*, 2103.
(4) Wagner, M. *Abstracts of Papers*, 225th National Meeting of the American Chemical Society, New Orleans, LA, Mar 23−27, 2003; American Chemical Society: Washington, DC, 2003; INOR 334.
(5) Batten, S. R.; Jeffery, J. C.; Ward, M. D. *Inorg. Chim. Acta* **1999**, *292*, 231.
(6) Xie, Y.; Wu, B. M.; Xue, F.; Ng, S. C.; Mak, T. C. W.; Hor, T. S. A. *J. Organomet. Chem.* **1997**, *531*, 175.
(7) Heeger, A. J. *Angew. Chem., Int. Ed.* **2001**, *40*, 2591. Levi, M. D.; Gofer, Y.; Aurbach, D. *Polym. Adv. Technol.* **2002**, *13*, 697.
(8) Levi, M. D.; Gofer, Y.; Aurbach, D. *Polym. Adv. Technol.* **2002**, *13*, 697.
(9) Gan, K. S.; Hor, T. S. A. *Ferrocene-Homogeneous Catalysis, Organic Syntheses and Materials Science*; Togni, A., Hayashi, T., Eds.; VCH: Weinheim, 1995; Chapter 1, p 3.
(10) Colacot, T. J.; Qian, H.; Olivares, R. C.; Ortega, S. H. *J. Organomet. Chem.* **2001**, *637*, 697.



10.1021/ic034690u CCC: $25.00 
Published on Web 09/27/2003

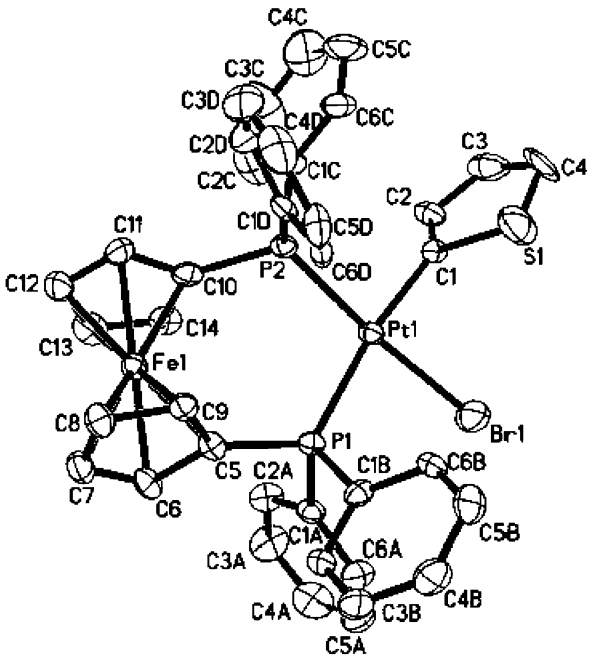


**Figure 1.** ORTEP drawing (50% probability ellipsoids) of the molecular structure of PtBr(dppf)($C_4H_3S$), **1**. The hydrogen atoms and solvent molecules are omitted for clarity.

**Table 1.** Selected Bond Distances (Å) and Angles (deg) of **1** and **2**

| | **1** | **2** |
|---|---|---|
| Pt(1)−Br(1) | 2.4707(10) | 2.4759(10) |
| Pt(1)−P(1) | 2.333(2) | 2.345(2) |
| Pt(1)−P(2) | 2.240(2) | 2.232(2) |
| Pt(1)−C(1) | 2.048(10) | 2.042(7) |
| Pt(2)−Br(2) | | 2.4760(11) |
| Pt(2)−P(3) | | 2.336(2) |
| Pt(2)−P(4) | | 2.234(2) |
| Pt(2)−C(8) | | 2.036(7) |
| C(1)−Pt(1)−P(2) | 88.6(3) | 84.0(2) |
| C(1)−Pt(1)−P(1) | 171.0(3) | 171.1(2) |
| P(2)−Pt(1)−P(1) | 100.36(8) | 102.81(8) |
| C(1)−Pt(1)−Br(1) | 85.4(3) | 87.0(2) |
| P(2)−Pt(1)−Br(1) | 85.63(6) | 168.75(6) |
| P(1)−Pt(1)−Br(1) | | 86.91(6) |
| C(8)−Pt(2)−P(3) | | 170.7(3) |
| C(8)−Pt(2)−P(4) | | 87.7(3) |
| P(4)−Pt(2)−P(3) | | 101.28(8) |
| C(8)−Pt(2)−Br(2) | | 86.3(3) |
| P(4)−Pt(2)−Br(2) | | 173.40(6) |
| P(3)−Pt(2)−Br(2) | | 84.90(6) |

(2) Å) is significantly shorter than that opposite the bithiophene (2.345(2) Å) group (Table 1). Similar spectroscopic and crystallographic patterns were observed for **1**, which is a mononuclear Pt(II) square planar complex with terminal bromide and thienyl and chelating dppf (Figure 1; Table 1). Similarly, the thienyl is a C-donor with a free sulfur end, which is known to be weakly basic.[11] Unlike the $PPh_3$ analogue, in which the phosphines are *trans*-oriented, both **1** and **2** adopt a *cis* configuration, which is geometrically imposed by the chelating dppf.

The *anti* orientation of the two dppf ligands in **2** keeps steric repulsion to its minimum. It also directs a similar *anti* orientation for the bromides. Although this cannot be understood as the absolute structure in solution, it nevertheless points to a possible source for Pt−bithienyl polymer or cyclic frameworks upon bromide replacement with other bidentate ligands. In principle, such anion exchange could proceed in parallel but opposite (*anti*) orientation, taking into consideration the role of anions, solvent, etc.[12]

To examine the potential for **2** in polymer synthesis, we studied its exchange behavior with an incoming nucleophile. An anionic, bifunctional, and heterocyclic ligand such as isonicotinate ($O_2CC_5H_4N$)[13] (abbreviated as isonic) was chosen. Complex **2** was found to be sluggish toward isonic and acetate (OAc) ($H^+$, $Na^+$, or $K^+$ form), even in the presence of a strong base (KOH) or under reflux conditions. However, with AgOAc, it reacts almost instantaneously to give the expected diacetate product. Monosubstitution cannot be achieved through stoichiometric control. Reaction of **2** with $Ag^+$ salts (e.g., $OTf^-$ = triflate) in $CH_3CN$ gives the solvent complex $[Pt_2(dppf)_2(\mu_2\text{-}C_8H_4S_2)(MeCN)_2]^{2+}2OTf^-$, **3**, which cannot be isolated as a solid. The mass spectroscopic analysis of **3** showed that **3** is dinuclear in solution. Thus, **3** can be used in situ to generate other substitution products. For example, with isonic ($K^+$) in acetone, it initially gave a yellow solid which, upon further addition of acetone dropwise, swelled to a brown lump. Upon addition of large excess of acetone, it turned into a pale brown gelatinous precipitate, whose $^{31}P$ NMR spectrum (acetone) showed, unexpectedly, four resonances with respective Pt satellites. This spectral pattern is inconsistent with the expected di-isonic (O-coordinated) product, viz. $[Pt_2(isonic)_2(dppf)_2(\mu_2\text{-}C_8H_4S_2)]$, but supports an O,N-isonic bridged polymeric product $[Pt_2(isonic)(dppf)_2(\mu_2\text{-}C_8H_4S_2)]_n^{n+}nOTf^-$. Unfortunately, its limited solubility precludes further characterization. Use of free isonicotinic acid (isonic$H^+$) with **3** gave an unexpected product **4**, with no evidence of bithienyl presence, but with successful introduction of the isonic group ($\nu_{COOasym}$ 1647 and 1637 $cm^{-1}$).[14] $^{31}P$ NMR analysis at room temperature (rt) (300 K) showed a major product with two mutually coupled resonances ($\delta$ 9.1, 5.4 ppm), and a pair of much weaker neighboring peaks with similar P−Pt couplings. At 213 K, the minor product disappeared leaving behind the major species (9.9, 6.6 ppm) in a clean spectrum (Figure 3). The original spectrum was restored when the temperature returned to rt. The Pt−P couplings (3755 and 3489 Hz) are significantly different from those of the starting bithienyl complex (1976, 4192 Hz), and there is also a significant high-field shift (9.1 and 5.4 vs 13.6 and 12.7 ppm in **2**). These point to the conservation of a molecular square framework (see in a following paragraph) within the temperature range 213−300 K.

These spectral features suggested that a new ligand environment is present. This could be achieved if both bromide and bithienyl are replaced by the N- and O-bonded isonic groups. Subsequent single-crystal crystallographic analysis proved this and revealed the formation of an unusual

(11) Chen, B. L. Synthesis and characterization of thiophene derivatives and their metal complexes. Ph.D. Thesis, National University of Singapore, 1999.

(12) Fujita, M. *Chem. Soc. Rev.* **1998**, *27*, 417.
(13) Song, R.; Kim, K. M.; Sohn, Y. S. *Inorg. Chim. Acta* **1999**, *292*, 238.
(14) Nakamoto, K. *Infrared and Raman Spectra of Inorganic and Coordination Compounds*, 4th ed.; Wiley: New York, 1986.

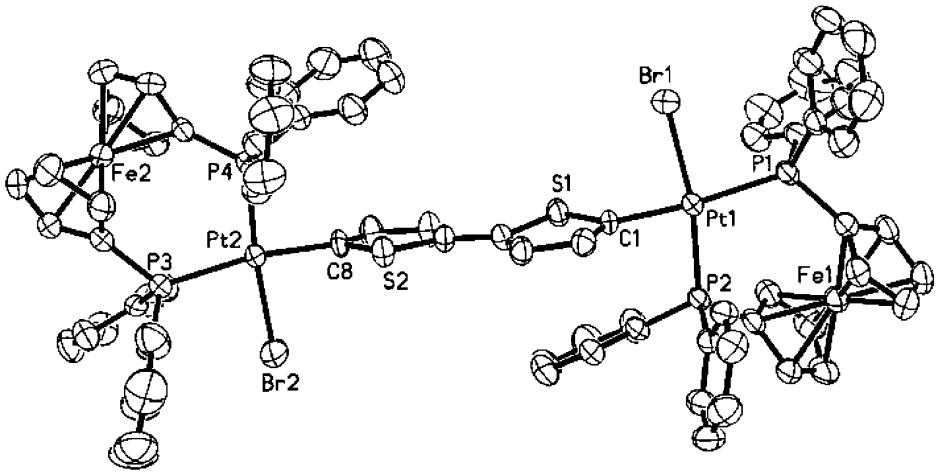


**Figure 2.** ORTEP drawing (50% probability ellipsoids) of the molecular structure of $Pt_2Br_2(dppf)_2(\mu_2\text{-}C_8H_4S_2)$, **2.** The hydrogen atoms and solvent molecules are omitted for clarity.

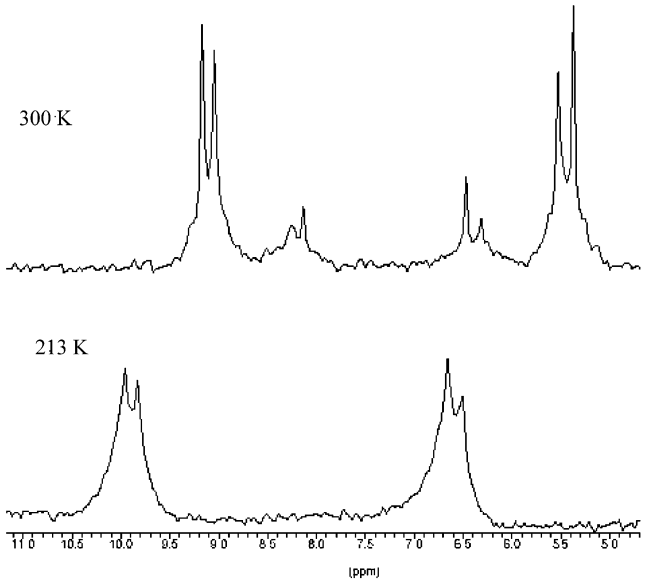


**Figure 3.** Variable temperature $^{31}P$ NMR spectra of the product from the reaction between **3** and isonic$H^+$, giving **4**, $[Pt_4(\mu_2\text{-isonic})_4(dppf)_4]^{4+}4OTf^-$.

macrocyclic structure, $[Pt_4(\mu_2\text{-isonic})_4(dppf)_4]^{4+}4OTf^-$, **4**, with four isonic groups bridging four metals through the pyridyl N and carboxyl O donors (Figure 4, Table 2). The coordination sphere at each Pt(II) center is completed by a chelating dppf. Since the local geometry of each Pt(II) is square planar, and they fuse through four bridging groups in a system that has no terminal ligand, this effectively is a macrocyclic molecular square assembled from four molecular subsquares. Effectively, we therefore witness an "all-ring" system with good $C_4$ symmetry. The isonic coordination mode is different from that observed by Sohn et al. who reported an N-coordination (to Pt(II)) to give zwitterions.[12] Rendina et al. reported isonicotic acids bridging platinum phosphine groups through H-bonds[15,16] to give dimeric or macrocyclic compounds. Compound **4** is different, in which the acid group is deprotonated. The carbonyl O atom (C═O) is noncoordinating in the macrocyclic compound (**4**) as compared to the bidentate carboxylate bridge formation reported in other macrocyclic complexes.[17] The quality of the crystallographic data of **4** does not permit any meaningful

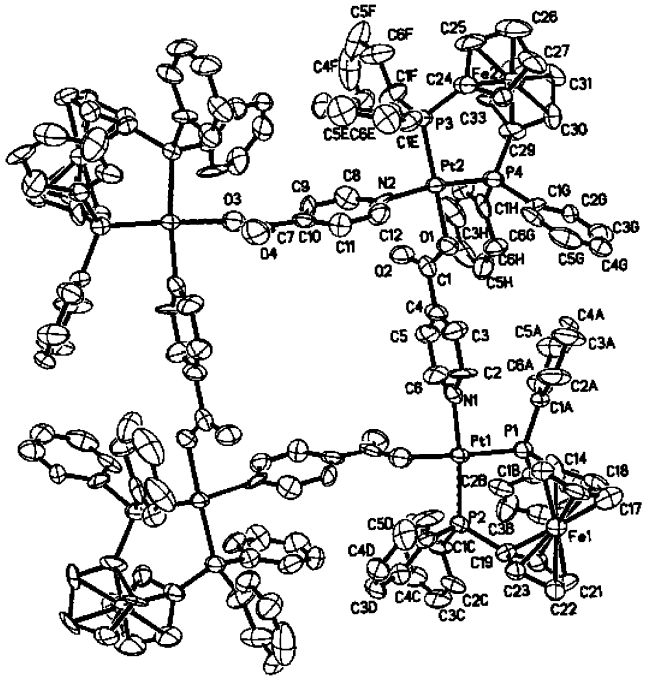


**Figure 4.** ORTEP drawing (50% probability ellipsoids) of the molecular structure of $[Pt_4(\mu_2\text{-isonic})_4(dppf)_4]^{4+}4OTf^-$, **4**. The hydrogen atoms and solvent molecules are omitted for clarity.

**Table 2.** Selected Bond Distances (Å) and Angles (deg) of **4**

| bond length | | bond angles | |
|---|---|---|---|
| Pt(1)−N(1) | 2.068(18) | N(1)−Pt(1)−O(3) | 86.5(6) |
| Pt(1)−O(3) | 2.093(15) | N(1)−Pt(1)−P(1) | 91.1(5) |
| Pt(1)−P(1) | 2.252(6) | O(3)−Pt(1)−P(1) | 176.4(4) |
| Pt(1)−P(2) | 2.287(5) | N(1)−Pt(1)−P(2) | 172.1(5) |
| Pt(2)−O(1) | 2.042(14) | O(3)−Pt(1)−P(2) | 86.2(4) |
| Pt(2)−N(2) | 2.062(19) | P(1)−Pt(1)−P(2) | 96.1(2) |
| Pt(2)−P(3) | 2.252(6) | O(1)−Pt(2)−N(2) | 87.0(6) |
| Pt(2)−P(4) | 2.263(6) | O(1)−Pt(2)−P(3) | 170.9(5) |
| | | N(2)−Pt(2)−P(3) | 88.5(4) |
| | | O(1)−Pt(2)−P(4) | 84.0(4) |
| | | N(2)−Pt(2)−P(4) | 169.8(5) |
| | | P(3)−Pt(2)−P(4) | 101.1(2) |

(15) Crisp, M. G.; Tiekink, E. R. T.; Rendina, L. M. *Inorg. Chem*. **2003**, *42*, 1057.
(16) Gianneschi, N. C.; Tiekink, E. R. T.; Rendina, L. M. *J. Am. Chem. Soc*. **2000**, *122*, 8474.

**Scheme 1.** Synthesis of $[Pt_4(\mu_2\text{-isonic})_4(dppf)_4]^{4+}4OTf^-$ **4**

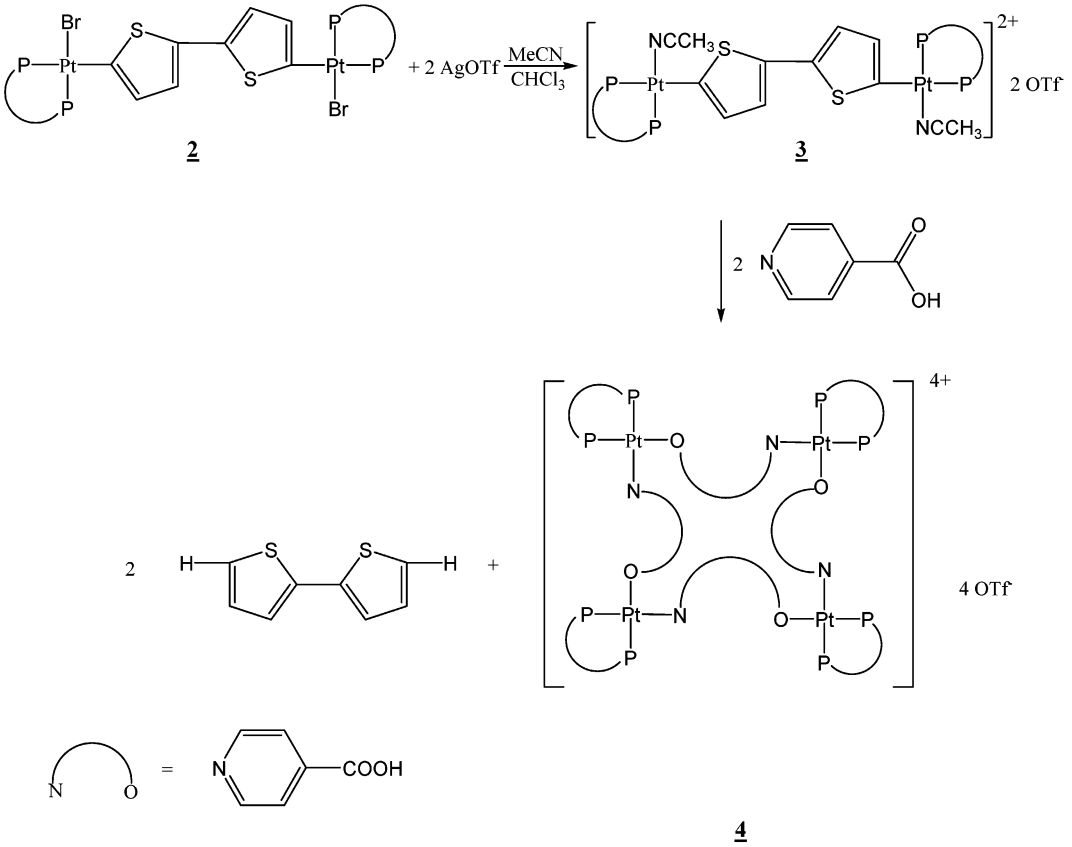


structural discussion in detail, but the molecular structure is without question. It also reveals some insight into the formation pathway. The acidic isonic$H^+$ helps to liberate bithienyl in form of bithiophene which then facilitates the ligand replacement (Scheme 1). The *trans* orientation of the O,N functional groups of the incoming ligand and the square planarity of the metal collectively help to assemble this molecular square architecture. The chelating dppf thus completes an "all-ring" formation. The side product observed in solution at rt therefore likely arises from other molecular geometries with the same stoichiometry and architecture. The square is the self-assembled thermodynamic product as it represents a good balance of entropy and geometry influences. The inequivalent phosphines with similar Pt−P couplings can then be explained by their *trans* orientation to two different but similarly hard ligands. In the crystal packing diagram (Figure 5), the molecular squares stack on top of each other, without any identifiable solvate trapped within the molecular ring.

The reaction between **1** and AgOTf in MeCN proceeds by a completely different pathway. It resulted in a yellow air-stable solid which redissolves in $CHCl_3$ to give an orange solution and, within minutes, a white gel. Upon standing overnight, orange crystals formed. Single-crystal crystallographic analysis (**5**) showed another unusual and unexpected six-membered $\{Pt_2C_2S_2\}$ ring formed by the fusion of two platinum−thienyl moieties through the S atoms. This

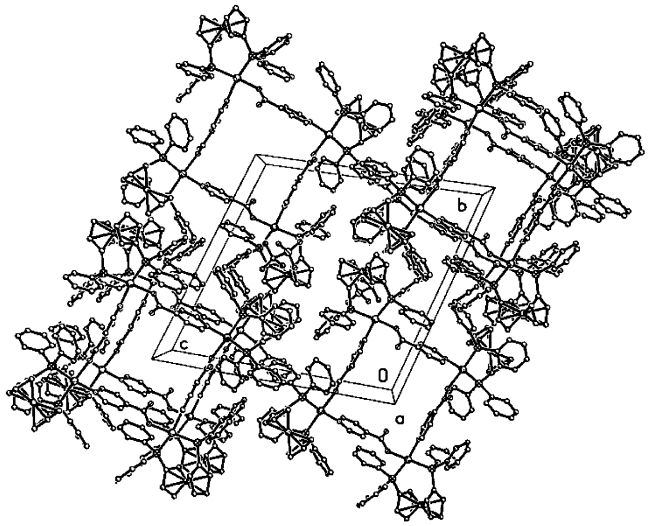


**Figure 5.** Molecular packing diagram of **4**.

is the only example in our study that shows S-coordination of a thiophene or thienyl group. This sulfur center in a conjugated system is notoriously weakly basic.[11,18,19] The metal-coordination, e.g., $\eta^5$, has precedent but is rare.[20] $\sigma$-Coordination through sulfur from thiophenes to transition metals is even less common.[21,22] To our knowledge, this is

(17) Bera, J. K.; Smucker, B. W.; Walton, R. A.; Dunbar, K. R. *Chem. Commun*. **2001**, *24*, 2562.
(18) Xie, Y.; Wu, B. M.; Xue, F.; Ng, S. C.; Mak, T. C. W.; Hor, T. S. A.; *Organometallics* **1998**, *17*, 3988.
(19) Angelici, R. J. *Coord. Chem. Rev*. **1990**, *105*, 61.
(20) Veiros, L. F. *J. Organomet. Chem*. **2001**, *632*, 3.
(21) Draganjac, M.; Ruffing, C. J.; Rauchfuss, T. B. *Organometallics* **1985**, *4*, 1909.

**Scheme 2.** Possible Synthetic Route to **5**, $[Pt_2(dppf)_2(\mu_2,\eta^1(C),\eta^1(S)\text{-}C_4H_3S)_2]^{2+}2OTf^-$

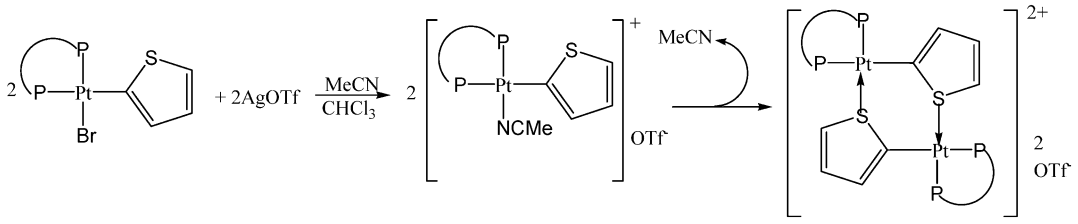


**1** **5**

the first example of C,S-bidentate coordination of thienyl. The facile formation of **5** can be explained by the generation of $[Pt(\eta^1(C2)\text{-}C_4H_3S)(dppf)(MeCN)]^+OTf^-$ (Scheme 2). This C-bonded thienyl complex could release the solvate (in the evaporation process) and dimerize as a result of coordination unsaturation of the metal. The proximity of the sulfur ensures a rapid dimerization process, which compensates for the solvent loss. It also explains our futile attempts to isolate the intermediate MeCN complex. Effectively, the two halves of the molecule are brought together by three fused rings comprising a six-membered $Pt_2C_2S_2$ metallo-ring sandwiched by two five-membered heterocyclic rings (Figure 6). The Pt−S bonds (av 2.398(3) Å) are typical of covalent Pt−S interaction[23−25] and comparable to those in other reported Pt−S rings (cf. 2.332 (4) Å[22] and 2.369(2), 2.351(2) Å[23]) (Table 3).

The stability of the $[Pt_4(isonic)_4]$ square and the $[Pt_2(thienyl)_2]$ ring is being studied, together with the construction of other unusual molecular geometries from our substrates. The thienyl and bithienyl systems have turned out to be very fruitful, not only as precursors to bifunctional coordination polymers but also in terms of the flexibility of functional replacement and sulfur involvement. These are unusual features that help pave our immediate path for new directions in molecular assemblies.

## Experimental Section

**General Procedures.** All reactions were performed under pure dry nitrogen using standard Schlenk techniques. The products are air-stable, and hence, recrystallizations were performed in air. All solvents and reagents were of reagent grade obtained from commercial sources and used without further purification. $Pt(PPh_3)_4$[26] and $PtBr(2\text{-thienyl})(PPh_3)_2$[6] were prepared according to literature methods.

All $^1H$ and $^{31}P$ NMR spectra were recorded at ca. 300 K at operating frequencies of 299.96 and 121.49 MHz, respectively. $^1H$ and $^{31}P$ chemical shifts are quoted in ppm downfield of $Me_4Si$ and 85% $H_3PO_4$, respectively. All IR spectra were recorded in the solid state on a Bio-Rad FT-IR spectrometer using KBr disk. Elemental analyses and Mass Spectrometry were performed by the Elemental Analysis Laboratory and Mass Spectrometry Laboratory of our department.

(22) Amari, C.; Ianelli, S.; Pelizzi, C.; Predieri, G. *Inorg. Chim. Acta* **1993**, *211*, 89.
(23) Meiji, R.; Stufkens, D. J.; Vrieze, K.; Roosendaal, E.; Schenk, H. *J. Organomet. Chem.* **1978**, *155*, 323.
(24) Jones, R.; Williams, D. J.; Wood, P. T.; Woollins, J. D. *Polyhedron* **1987**, *6*, 539.
(25) Albano, V. G.; Monari, M.; Orabona, I.; Panunzi, A.; Roviello, G.; Ruffo, F. *Organometallics* **2003**, *22*, 1223.
(26) Ugo, R. *Inorg. Synth.* **1968**, *11*, 105.

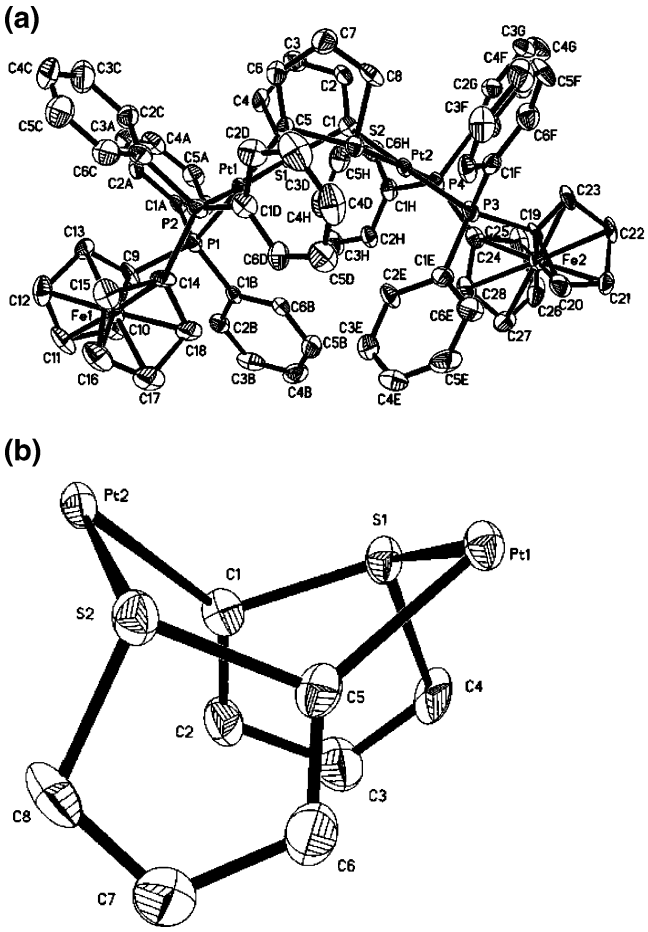


**Figure 6.** (a) ORTEP drawing (50% probability ellipsoids) of the molecular structure of **5**, $[Pt_2(dppf)_2(\mu_2,\eta^1(C),\eta^1(S)\text{-}C_4H_3S)_2]^{2+}2OTf^-$. The hydrogen atoms and solvent molecules are omitted. (b) The central three-ring region is expanded for clarity.

**Table 3.** Selected Bond Distances and Angles of **5**

| bond length | | bond angle | |
|---|---|---|---|
| Pt(1)−C(5) | 2.067(10) | C(5)−Pt(1)−P(2) | 85.6(3) |
| Pt(1)−P(2) | 2.277(3) | C(5)−Pt(1)−P(1) | 172.2(3) |
| Pt(1)−P(1) | 2.350(3) | P(2)−Pt(1)−P(1) | 101.19(9) |
| Pt(1)−S(1) | 2.396(3) | C(5)−Pt(1)−S(1) | 86.4(3) |
| Pt(2)−C(1) | 2.012(10) | P(2)−Pt(1)−S(1) | 172.01(9) |
| Pt(2)−P(3) | 2.343(3) | P(1)−Pt(1)−S(1) | 86.80(9) |
| Pt(2)−S(2) | 2.400(3) | C(1)−Pt(2)−P(4) | 85.4(3) |
| | | C(1)−Pt(2)−P(3) | 172.6(3) |
| | | P(4)−Pt(2)−P(3) | 101.56(10) |
| | | C(1)−Pt(2)−S(2) | 86.7(3) |
| | | P(4)−Pt(2)−S(2) | 171.93(9) |
| | | P(3)−Pt(2)−S(2) | 86.41(9) |

**Syntheses. Synthesis of $Pt(dppf)(C_4H_3S)Br$, 1.** $PtBr(C_4H_3S)(PPh_3)_2$ (0.4414 g, 0.5 mmol) dissolved in $CH_2Cl_2$ (20 mL) to give a colorless solution, upon which dppf (0.2772 g, 0.5 mmol) was added. The resultant yellow solution was concentrated to ca. 3 mL

**Table 4.** Crystallographic Data and Refinement Details for **1**, **2**, **4**, and **5**

| | **1**[a] | **2** | **4** | **5** |
|---|---|---|---|---|
| empirical formula | $(C_{38}H_{31}BrFeSPt \times 0.9) + (C_{34}H_{28}Br_2FePt \times 0.1) + CH_2Cl_2$ | $C_{81}H_{65}Br_2Cl_{15}Fe_2P_4Pt_2S_2$ | $C_{165}H_{129}Cl_3F_{12}Fe_4N_4O_{24}P_8Pt_4S_4$ | $C_{84}H_{68}Cl_{18}F_6Fe_2O_6P_4Pt_2S_4$ |
| $T$ (K) | 223 (2) | 223 (2) | 223 (2) | 223 (2) |
| fw | 997.08 | 2419.78 | 4265.83 | 2679.48 |
| cryst syst | monoclinic | monoclinic | triclinic | triclinic |
| space group | $P2_1/c$ | $P2_1/c$ | $P1$ | $P1$ |
| unit cell dimensions | | | | |
| $a$ (Å) | 22.8672 (13) | 17.9506 (10) | 13.081 (3) | 14.0474 (9) |
| $b$ (Å) | 9.4384 (5) | 17.2014 (10) | 19.233 (4) | 14.3402 (9) |
| $c$ (Å) | 16.4891 (10) | 29.4006 (17) | 20.302 (4) | 26.0749 (17) |
| α (deg) | 90 | 90 | 101.189 (4) | 99.2230 (10) |
| $\beta$ (deg) | 104.6670 (10) | 97.1910 (10) | 105.355 (4) | 100.7800 (10) |
| $\gamma$ (deg) | 90 | 90 | 105.829 (4) | 97.7680 (10) |
| $V$ (Å$^3$) | 3442.9 (3) | 9006.8 (9) | 4539.3 (15) | 5018.8 (6) |
| $Z$ | 4 | 4 | 1 | 2 |
| $D_{calcd}$ (mg/m$^3$) | 1.924 | 1.784 | 1.560 | 1.773 |
| abs coeff (mm$^{-1}$) | 6.089 | 4.904 | 3.614 | 3.748 |
| $F$(000) | 1941 | 4704 | 2098 | 2624 |
| cryst size (mm$^3$) | 0.36 × 0.10 × 0.08 | 0.30 × 0.25 × 0.20 | 0.14 × 0.08 × 0.04 | 0.40 × 0.28 × 0.16 |
| index ranges | $-27 \le h \le 27$, $-11 \le k \le 11$, $-12 \le l \le 19$ | $-21 \le h \le 20$, $-20 \le k \le 20$ $-17 \le l \le 34$ | $-15 \le h \le 15$, $-22 \le k \le 22$, $-24 \le l \le 24$ | $-16 \le h \le 16$, $-17 \le k \le 17$, $-31 \le l \le 31$ |
| $R$, wR2 (all data) | 0.0623, 0.1301 | 0.0617, 0.1186 | 0.2245, 0.3014 | 0.0968, 0.1548 |
| final $R$, wR2 | 0.0505, 0.1244 | 0.0438, 0.1111 | 0.1064, 0.2490 | 0.0673, 0.1446 |
| largest diff peak and hole (e Å$^{-3}$) | 2.634 and −2.055 | 1.493 and −0.793 | 2.734 and −2.047 | 2.239 and −2.846 |

[a] Compound **1** = 0.9[PtBr(2-thienyl)(dppf)] + 0.1[$PtBr_2$(dppf)] + $CH_2Cl_2$.

in vacuo, and $Et_2O$ was added to precipitate a yellow solid. Upon isolation, it was washed with $Et_2O$ and dried in vacuo. Recrystallization from $CH_2Cl_2$/hexane gave yellow crystals (80%). $^1$H NMR: $\delta$ = 8.0, 7.9, 7.5, 7.3, 7.2(m), 6.6(d), 6.2(t), 4.7(t), 4.5(s), 4.1(d), 3.7(t). $^{31}$P NMR: $\delta$ = 13.6(d), 13.2(d) $^2J_{P-P}$ = 15.26 Hz, $^1J_{P-Pt}$ = 2006.58, 4135.22 Hz. ESI: $m/z$ = 832.1 (100%) [**1** − Br]$^+$. Anal. Calcd for 90% $C_{38}H_{31}P_2SBrFePt$ + 10% $C_{34}H_{28}P_2Br_2FePt$: C, 49.50; H, 3.39; S, 3.16. Found: C, 49.05; H, 3.31; S, 2.78.

**Synthesis of $Pt_2Br_2(dppf)_2(\mu_2\text{-}C_8H_4S_2)$, 2.** 5,5′-Dibromo-2,2′-bithiophene (0.4051 g, 1.25 mmol) was added to a solution of $Pt(PPh_3)_4$ (3.1104 g, 2.5 mmol) in toluene. After 15 h of reflux, a pale yellow precipitate was obtained. $Et_2O$ was added to complete the precipitation. Filtration gave a solid which was washed with $Et_2O$ and dried in a vacuum to give a pale yellow solid (90%). This solid (0.2645 g; 0.15 mmol) was added to toluene (30 mL) to give a yellow mixture, upon which dppf (0.1663 g, 0.3 mmol) was added. The resultant mixture was refluxed overnight to give a bright yellow mixture, upon which $Et_2O$ was added. The precipitate was filtered, washed with $Et_2O$ and dried in vacuo to give a bright yellow solid product (87%). $^{31}$P NMR: $\delta$ = 13.6 (d), 12.7 (d), $^2J_{P-P}$ = 15.26 Hz, $^1J_{P-Pt}$ = 1976, 4192 Hz. $^1$H NMR: $\delta$ = 8.1, 7.5, 7.3, 7.1(m), 6.3 (d), 5.9 (d), 4.7(s), 4.4(s), 4.1(s), 3.7(s). FAB: $m/z$ = 1823.0 (25%) (molecular ion, M$^+$ peak), 1743.0 (25%) [**2** − Br]$^+$, 831 (40%) [**2** − 2Br]$^{2+}$. Compound **2** was recrystallized in $CHCl_3$/hexane to give orange crystals. Anal. Calcd for $C_{76}H_{60}P_4S_2Br_2Fe_2Pt_2$·2$CHCl_3$: C, 45.43; H, 3.18; S, 3.10. Found: C, 45.96; H, 3.03; S, 3.10. Some chloroform as appeared in the X-ray crystals has been lost in the process of drying the samples for elemental analysis.

**Synthesis of $[Pt_2(dppf)_2(\mu_2\text{-}C_8H_4S_2)(MeCN)_2]^{2+}$ 2OTf$^-$, 3.** AgOTf (0.0129 g, 0.05 mmol) was dissolved in MeCN (3 mL) shielded from light followed by the addition of acetone (15 mL). Complex **2** (0.0456 g 0.025 mmol) was added to the solution to give a yellow suspension. The mixture was stirred until the solution turned clear yellow with an off-white precipitate, which was removed by filtration over a column of Celite. The filtrate was condensed and spectroscopically analyzed. $^{31}$P NMR: $\delta$ = 19.6-(d), 8.6(d) ppm; $^1J_{P-Pt}$ = 2068, 4396 Hz. ESI: $m/z$ = 831.5 (100%) [**3** − 2MeCN]$^{2+}$. A sharp singlet at 10.7 ppm, $^1J_{P-P}$ = 4433 Hz, and some fine peaks are observed in the $^{31}$P NMR when the solid product was isolated and redissolved in $CDCl_3$. The identities of the decomposed products are not known.

**Synthesis of $[Pt_4(\mu_2\text{-isonic})_4(dppf)_4]^{4+}$4OTf$^-$, 4.** AgOTf (0.0129 g, 0.05 mmol) was dissolved in MeCN (3 mL), and $CHCl_3$ (15 mL) was added, followed by **2** (0.0456 g, 0.025 mmol). A clear yellow solution with an off-white precipitate formed immediately. The mixture was stirred for 45 min and filtered. IsonicH$^+$ (0.0062 g, 0.05 mmol) was added to the filtrate, and the mixture stirred for 5 h. A white suspension in a yellow solution was obtained. The mixture was filtered and the filtrate condensed to ca. 3 mL. $Et_2O$ was added to precipitate the product. Careful recrystallization in $CHCl_3$/hexane gave yellow triclinic crystals (64%). $^{31}$P NMR (213 K): $\delta$ = 9.9(d), 6.6(d); $^2J_{P-P}$ = 15.26 Hz, $^1J_{P-Pt}$ = 3755, 3489 Hz. $^1$H NMR (213 K): $\delta$ = 8.5(s) (pyridyl H), 7.8, 7.5, 7.3, 7.0-(m) (phenyl H), 4.6, 4.5, 4.4, 4.3(s) (Cp). IR/cm$^{-1}$: $\nu(COO)_{asym}$, 1647, 1637; $\nu(COO)_{sym}$, 1342. ESI: $m/z$ = 871.0 (100%) (molecular ion, M$^{4+}$). Anal. Calcd for $C_{164}H_{128}P_8O_{20}N_4F_{12}S_4Fe_4Pt_4$·2$CHCl_3$·4$H_2O$: C, 45.75; H, 3.19; N, 1.29; S, 2.94. Found: C, 45.72; H, 3.20; N, 0.78; S, 3.43. Some chloroform as appeared in the X-ray crystals has been lost in the process of drying the samples for elemental analysis.

When **3** was reacted with potassium isonicotinate, the solution remained yellow after overnight stirring. A yellow precipitate was obtained when $Et_2O$ was added to the condensed solution. The solid dissolved in acetone (a few drops) to give a swollen brown lump, and on addition of excess acetone, a yellow solution with pale brown gelatinous precipitate was obtained. $^{31}$P of solid product in $CD_3COCD_3$: $\delta$ = 23.5(t), 20.3(t), 7.5(t), 3.1(t); $^2J_{P-P}$ = 15.25 Hz, $^1J_{P-Pt}$ = 2109, 2091, 4209, 3649 Hz.

**Synthesis of $[Pt_2(dppf)_2(\mu_2,\eta^1(C),\eta^1(S)\text{-}C_4H_3S)_2]^{2+}$2OTf$^-$, 5.** AgOTf (0.0128 g, 0.05 mmol) was dissolved in MeCN (3 mL), followed by addition of $CHCl_3$ (15 mL). Complex **1** (0.0456 g,

0.05 mmol) was added to give a clear yellow solution with an off-white precipitate of AgBr. The mixture was stirred for 30 min and filtered to give a clear yellow filtrate, which was condensed to ca. 3 mL, and $Et_2O$ added to give a yellow precipitate. This precipitate was redissolved in $CHCl_3$ to give an orange solution which, upon standing, gave a white gel in the orange solution. Orange crystals were obtained when this mixture was left to stand overnight. $^{31}P$-NMR analysis of the gel mixture showed a sharp singlet at 9.1 ppm, $^1J_{P-Pt} = 3941$ Hz and 2 small doublets at 11.4, 14.7 ppm, $^2J_{P-P} = 15.26$ Hz, $^1J_{P-Pt} = 3685$, 4219 Hz. The identities of these decomposed materials are unknown. The limited solubility of the crystals did not allow further solution studies. Anal. Calcd for $C_{78}H_{62}P_4S_4O_6F_6Fe_2Pt_2 \cdot CHCl_3$: C, 45.55; H, 3.05; S, 6.16. Found: C, 45.07; H, 3.14; S, 3.79. Some chloroform as appeared in the X-ray crystals has been lost in the process of drying the samples for elemental analysis.

**Crystal Structure Determinations.** The diffraction experiments were carried out on a Bruker SMART CCD diffractometer with a Mo K$\alpha$ sealed tube at $-50$ °C. The program SMART[27] was used for collecting frames of data, indexing reflections, and determining lattice parameters, SAINT[26] for integration of the intensity of reflections and scaling, SADABS[28] for absorption correction, and SHELXTL[29] for space group and structure determination and least-squares refinements on $F^2$. The relevant crystallographic data and refinement details are shown in Table 4. Compound **2** crystallized with five molecules of $CHCl_3$. Compound **1** crystallized with one $CH_2Cl_2$ molecule. Good single crystals were difficult to obtain. The one chosen for X-ray analysis was disordered at the thienyl ring. The resulting best model showed that about 10% of the thienyl group was replaced by Br; i.e., the crystal contained 90% compound **1** and 10% $PtBr_2$(dppf) as impurity. The presence of residual $PtBr_2$-(dppf) was supported by a small singlet observed at 12.3 ppm in the $^{31}P$ NMR spectrum of **1**. Compound **4** crystallized with four triflate anions, four $CHCl_3$ molecules, and four $H_2O$ molecules. The $CHCl_3$ molecules were severely disordered, and a model with occupancy of 50:50 was resolved and included in the least squares refinement cycles. The size of the square gives a free space of ca. 4−5 Å, which is big enough to accommodate a small solvent molecule. However, the general background difference peaks are high due to the poor data quality. There is only one peak of 1.4 e/Å$^3$ inside the square. The other peaks inside the square are below 0.8 e/Å$^3$. On the basis of these, we could not ascertain or identify any solvent in the cavity, but it is probable that some fractional solvent molecules are trapped within during crystallization. The crystallographic data of **4** were poor due to the poor quality and small size of the crystal. Despite numerous attempts, we could not produce better crystals for reanalysis. Compound **5** crystallized with six $CHCl_3$ molecules, and two out of six of them were severely disordered with occupancy of 50:50 and 70:30.

(27) *SMART and SAINT Software Reference Manuals*, version 5.611; Bruker Analytical X-ray Systems, Inc.: Madison, WI, 2000.
(28) Sheldrick, G. M. *SADABS, software for empirical absorption correction*; University of Göttingen: Göttingen, Germany, 2000.
(29) *SHELXTL Reference Manual*, version 5.1; Bruker Analytical X-ray Systems, Inc.: Madison, WI, 1997.

**Acknowledgment.** We acknowledge the National University of Singapore for financial support and technical assistance from our department. We are grateful to F. Zhao for some supporting experiments.

**Supporting Information Available:** Crystallographic data in CIF format. This material is available free of charge via the Internet at http://pubs.acs.org.

IC034690U